STUDIA UBB PHYSICA, Vol. 67 (LXVII), 1-2, 2022, pp. 91-106
(RECOMMENDED CITATION)
doi:10.24193/subbphys.2022.08

RASHBA FIELD CONTRIBUTION AND ELECTRIC FIELD CONTROL OF THE MAGNETIC ANISOTROPY

R.-A. ONE[1], C. V. TIUSAN[1,2,*]

ABSTRACT. The anatomy of the Perpendicular Magnetic Anisotropy (PMA) in magnetic multilayered thin film heterostructures and the possibility to efficiently manipulate it by external electric fields represent major issues for technological applications in magnetic data storage devices. Solving a standard quantum model based on a Stoner-Rashba Hamiltonian, we illustrate that the magnetic properties in ultrathin magnetic films arise from the competing components identified in the magnetic energy: the Rashba correction to the Stoner splitting, a pseudo-dipolar contribution to the anisotropy energy proportional to the electric field at the interface that would favor in-plane magnetization configuration and a uniaxial-like perpendicular anisotropy term. This last term is responsible on the perpendicular magnetization configuration in ultrathin films and depends on the square of the electric field at the surface of the film. Investigating the time evolution of the magnetic system, we described the macrospin magnetization dynamics in terms of a Rashba field induced magnetization precession. Despite its simplicity, the quantum approach underlines the basic issues related to the physical origin and the mechanisms of the perpendicular magnetization in ultrathin magnetic films and illustrates the capability of manipulation by external gating electric field, in experiments similarly to Nuclear Magnetic Resonance.

Keywords: *perpendicular magnetic anisotropy, electric field control of anisotropy, magnetic tunnel junctions, magnetic multilayer heterostructures.*

[1] *Babeș-Bolyai University, Faculty of Physics, 1 M. Kogălniceanu, 400084 Cluj-Napoca, Romania*
[2] *National Center of Scientific Research (CNRS), France*
* *Corresponding author: coriolan.tiusan@ubbcluj.ro*

INTRODUCTION

The Perpendicular Magnetic Anisotropy (PMA) in ultrathin magnetic films represents nowadays one of the most developed experimental and theoretical topics in the magnetic data storage technologies. This is correlated to the enhanced thermal stability and the switching efficiency by spin-transfer-torque in magnetic random-access memories devices. A deep understanding of the fundamental physics related the PMA, its intrinsic anatomy and the possibility to control it by external stimuli (e.g. electric fields) in magnetic multilayer structures represents major issues for efficiently operating the magnetic random access memories (MRAM) devices [1]. Particularly, in case of ultrathin magnetic films, the magnetic anisotropy can be driven by interface effects. This opens the possibility of its control by external electric fields (E-field), that can be applied at the ferromagnetic film interface in cleverly designed spintronic device geometries. The non-zero interface electric fields affect the electronic properties of metallic interfaces and have a few monolayers penetration depth before vanishing by screening, when going in depth towards the bulk. Moreover, the ***E***-field control of the anisotropy provides enhanced energetic efficiency [2] for operating the spintronic devices. Extremely low energy consumption levels, of few fJ/bit [3,4] and sub-nanosecond switching times [5] have been already experimentally demonstrated.

Within these complex technological problematics, concerning the perpendicular magnetic anisotropy and its possibility to be manipulated, the basic understanding of the underlying physics represents a very important step. For describing the perpendicular magnetic anisotropy, often, more sophisticated *ab-initio* [6,7] and micromagnetic models are involved [8]. They underly electronic structure features responsible on the PMA: i.e., charge transfer and orbital population at the ferromagnetic metal/ insulator interface or interfacial Rashba field mechanisms illustrated by the bans structure analysis. On the other hand, the micromagnetic analysis incorporates other complex magnetic issues such as the magnetic anisotropy energy, its variation ratio with the electric field and magnetization damping phenomena. However, in this paper we illustrate that even a simple quantum model, based on a Stoner-Rashba Hamiltonian [9, 10] can be successfully used to depict major static and dynamic features related to the anatomy of the PMA in ultrathin films and its possibility to be toggled by external gating electric fields. The main results and predictions of this quantum analytical approach are in good qualitative agreement with the ones issued from more sophisticated DFT and micromagnetic calculations.

THEORETICAL MODEL, RESULTS AND DISCUSSION

In our paper, we develop a simple analytic quantum model based on the bi-dimensional Rashba contribution to the spin-orbit interaction and we show that this interaction is responsible on the perpendicular magnetic anisotropy. The magnetism (e.g., the exchange interaction) is introduced via a Stoner contribution to the Hamiltonian that competes with the Rashba spin-orbit fields. To build the Stoner-Rashba Hamiltonian, we add a Dirac spin orbit contribution that includes the spin-orbit effects to the band Stoner Hamiltonian. Therefore, in the total Hamiltonian (eq. 1) we easily recognize the kinetic free-electron contribution, the Stoner exchange, described in terms of an external molecular field J_0, and the Dirac spin orbit contribution containing the spin-orbit effects.

$$H_{SO} = \frac{\hat{p}^2}{2m} - J_0 \hat{m} \cdot \hat{\sigma} + \frac{\hbar}{2m_0 c^2} \vec{\nabla} V \cdot (\hat{\sigma} \times \hat{p}) \quad (1)$$

The third term describing the coupling between the electron spin and its orbital is deduced from the Dirac equation for a relativistic electron, expanded to the lowest order in $(v/c)^2$ (v and c are the electron and light velocities, respectively). A simple calculation (see Appendix 1) shows that for a central potential, the spin orbit contribution to the Hamiltonian describing the interaction between the carrier spin and the carrier momentum is proportional to the scalar product between the spin $\vec{S}$ and the orbital $\vec{L}$ angular moments (with λ being the spin-orbit interaction constant): $H_{SO} = \lambda \vec{L} \cdot \vec{S}$. This self-comprehensive expression for the SO-component in the Hamiltonian gives the name for the spin-orbit interaction.

In the Hamiltonian (1), m is the carrier (electron) mass, $\hbar$ the reduced Planck constant, $\hat{p} = \hbar \hat{k}$ is the momentum operator; the vector $\hat{m}$ is the magnetization $\vec{M}$ unit vector: $\hat{m} = \frac{\vec{M}}{M}$ with the components: $\hat{m}$ = (sinθ cosφ, sinθ sin φ, cos θ)- see figure 1 and $\hat{\sigma} = (\hat{\sigma}_x, \hat{\sigma}_y, \hat{\sigma}_z)$ is the operator of the Pauli spin matrices:

$$\hat{\sigma}_x = \begin{pmatrix} 0 & 1 \\ 1 & 0 \end{pmatrix}; \quad \hat{\sigma}_y = \begin{pmatrix} 0 & -i \\ i & 0 \end{pmatrix}; \qquad \hat{\sigma}_z = \begin{pmatrix} 1 & 0 \\ 0 & -1 \end{pmatrix};$$

related to the spin operator $\hat{S} = \frac{\hbar}{2}\hat{\sigma}$ and corresponding to the situation when the oz axis is the quantization axis for the magnetic field.

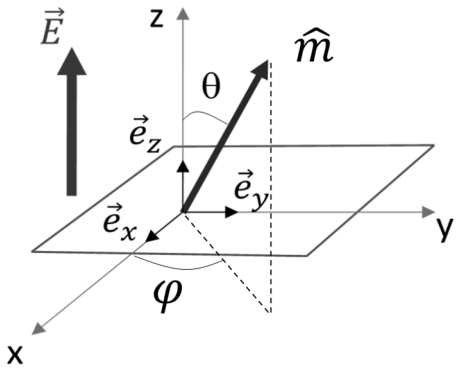

Figure 1

Geometry used in the analytical model, $\vec{e}_x$, $\vec{e}_y$, $\vec{e}_z$ are the unit vectors of ox, oy, oz axes. The electric field will be applied along the oz axis, perpendicular to the plane of the magnetic film.

The magnetic ultrathin film, having a thickness smaller than the mean free-electron path, can be reasonably assimilated to a two-dimensional electron gas (2DEG) in which the electrons are only moving within the xoy plane. Therefore, the electron wave vector will have only in-plane components $k_{II}=(k_x,k_y)$. Moreover, our model assumes that an electric field is applied perpendicular to this plane: $\vec{E} = (0,0,E_z)$. Later, we will reiterate that this field can be either an applied external field or an intrinsic electric field arising at the depletion zone when the ferromagnetic film is interfaced either with an insulator or with another metal (e.g., nonmagnetic) with different work-function or, the intrinsic field at the surface of the metallic film due to the symmetry breaking induced potential gradient. Within this model, considering the 2DEG with the confinement direction perpendicular to the propagation direction, we can calculate the vector product:

$$\hat{\sigma}\times\hat{p} = \begin{vmatrix} \hat{x} & \hat{y} & \hat{z} \\ \hat{\sigma}_x & \hat{\sigma}_y & \hat{\sigma}_z \\ p_x & p_y & p_z \end{vmatrix} \tag{2}$$

$$\hat{\sigma}\times\hat{p} = \hat{x}\left(p_z\hat{\sigma}_y - p_y\hat{\sigma}_z\right) - \hat{y}\left(p_z\hat{\sigma}_x - p_x\hat{\sigma}_z\right) + \hat{z}\left(p_y\hat{\sigma}_x - p_x\hat{\sigma}_y\right)$$

to find the expression of the Dirac third term in equation (1) within the hypothesis of our 2DEG model.

If the electric field $\vec{E} = -\nabla V$ is applied along the oz axis, perpendicular to the 2DEG plane, we have:

$$\vec{\nabla}V\cdot\left(\hat{\sigma}\times\hat{p}\right) = -\frac{\partial V}{\partial z}\left(\hat{p}_x\hat{\sigma}_y - \hat{p}_y\hat{\sigma}_x\right) \tag{3}$$

This would lead to the Stoner-Rashba Hamiltonian, which is the particular case of the Stoner-Dirac Hamiltonian in case of a 2DEG with an electric field applied perpendicular to the electron mobility plane:

$$\widehat{H} = \frac{\hat{p}^2}{2m} - J_0\hat{m}\cdot\hat{\sigma} + \frac{\alpha_R}{\hbar}\left(\hat{\sigma}_x\hat{p}_y - \hat{\sigma}_y\hat{p}_x\right) = \frac{\hbar^2\hat{k}^2}{2m} - J_0\hat{m}\cdot\hat{\sigma} + \alpha_R\left(\hat{\sigma}_x\hat{k}_y - \hat{\sigma}_y\hat{k}_x\right) \quad (4)$$

with $\alpha_R = \frac{\hbar^2}{2m_0c^2}\frac{\partial V}{\partial z}$ defining the Rashba coefficient. Because the electric field in our model has only a z component, we have: $\vec{E} = (0,0,E_z) \Longrightarrow \overrightarrow{\nabla V} = \frac{\partial V}{\partial z}\vec{e}_z$, which states that the Rashba coefficient is proportional with the z (perpendicular) component of the electric field.

This approach leads to the following immediate conclusions: (i) the larger is the electric-field felt by the electron, the larger is the SO-coupling; (ii) in case of an atom, the ***E***-field is proportional to the atomic number Z (***E***~Ze); this explains why the SO-coupling is larger for heavy atoms: Au (Z=79), Pt (Z=78), Pd (Z=46) than for 3d atoms: Cr (Z=24), Fe (Z=26),Co (Z=27), Ni (Z=28); (iii) the SO-coupling is exacerbated at the metal surfaces: i.e, the breaking of the translational symmetry in surface is equivalent to a potential gradient felt by the electron => electric field; (iv) in case when a metal-insulator (or metal semiconductor) interface is created in a multilayer heterostructure, a depletion zone appears with corresponding significant interfacial intrinsic electric field.

1. Stationary solution: eigenstates and eigenvalues

Within the Heisenberg-Dirac formalism, we solve the stationary Schrodinger equation by diagonalizing the spin-orbit Hamiltonian and find the eigenvalues and the stationary eigenfunctions.

The $\hat{k}_x$ and $\hat{k}_y$ wave vector operators commute with $\widehat{H}$, then the eigenfunctions of the system are:

$$\left|\Psi\right\rangle = e^{i(k_x x + k_y y)}\left(C_1\left|+\right\rangle + C_2\left|-\right\rangle\right) = e^{i\vec{k}_{\parallel}\vec{r}}\left(C_1\left|+\right\rangle + C_2\left|-\right\rangle\right) \quad (5)$$

The $\{|+\rangle, |-\rangle\}$ wave functions represent the up (UP) and down (DN) electron states of the *z* component of the spin (S_z), they are orthonormal and form

a basis. We remember that, in our model, the *z* direction in the electron referential is chosen to be the quantization direction of the effective magnetic field $\mathbf{B}_{\text{eff.}}$ leading to a diagonal $\hat{\sigma}_z$.

The eigenvalues are issued from diagonalizing the Hamiltonian matrix (See Appendix 2) whose components are calculated within the $\{|+\rangle, |-\rangle\}$ basis. After solving the eigenvalues problem within the Heisenberg matrix formalism, we get:

$$\varepsilon_{\pm} = \frac{\hbar^2 k^2}{2m} \mp \sqrt{J_0^2 + 2J_0 \alpha_R k_x \sin\theta + \alpha_R^2 k^2} \tag{6}$$

$$\text{or,} \quad \varepsilon_{\sigma} = \frac{\hbar^2 k^2}{2m} - \sigma J_0 \sqrt{1 + \frac{2\alpha_R k_x}{J_0} \sin\theta + \frac{\alpha_R^2 k^2}{J_0^2}}; \quad \sigma = \pm 1 \,(\text{UP, DN}) \tag{7}$$

A development in $\alpha k/J_0 \ll 1$ (that would correspond to the common experimental situation when the Rashba interaction is much smaller than Stoner interaction) leads to:

$$\varepsilon_{\sigma}(k) = \frac{\hbar^2 k^2}{2m} - \sigma J_0 \left(1 + \frac{1}{2}\frac{\alpha_R^2 k^2}{J_0^2}\right) - \sigma J_0 \frac{\alpha_R k_x}{J_0} \sin\theta + \frac{1}{2}\sigma J_0 \frac{\alpha_R^2 k_x^2}{J_0^2} \sin^2\theta \tag{8}$$

In this equation we identify the following contributions:

(1) the first kinetic term, corresponding to the free electron 2DEG with parabolic dispersion bands.
(2) the second term represents the Rashba correction to the Stoner splitting. The proportionality with α_R indicates a quadratic dependence of this contribution to the total energy with respect to the electric field.
(3) the third term represents pseudo-dipolar contribution to the anisotropy energy. It favors the in-plane magnetization (minimum when $\theta = \pi/2$). Because α_R depends linearly on the electric field, the in-plane pseudo-dipolar contribution to the anisotropy will depend linearly on the electric field.
(4) the fourth term corresponds to a uniaxial-like anisotropy. One can see that it favors the perpendicular to the film plane magnetization (energy minimum when $\theta = 0$). Following the square dependence in α_R, one can deduce that the pure Rashba mechanism induces a quadratic dependence of the uniaxial PMA with the electric field.

The eigenvalues dispersion described by the equation (8) can be depicted by the band diagrams $\varepsilon = \varepsilon_{\sigma}(k)$, schematically illustrated for both nonmagnetic (Fig. 2(a)) or magnetic case (Fig. 2(b)).

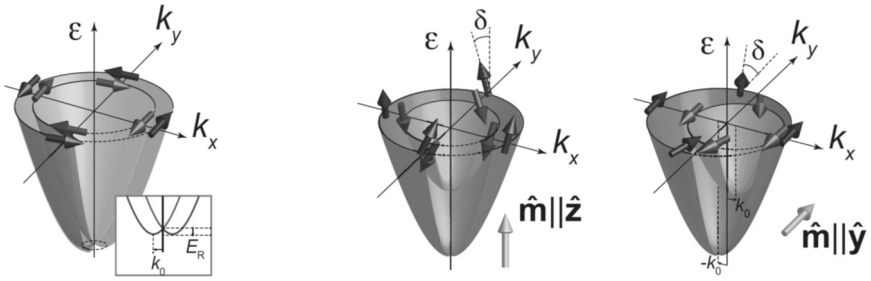

Figure 2. Band diagrams $\varepsilon = \varepsilon_\sigma(k)$ corresponding to a (a) nonmagnetic case (b) magnetic case, as issued from diagonalizing the Stoner-Rashba Hamiltonian -image adapted from [10]. From eq. (6) the dispersion relations in the nonmagnetic case are: $\varepsilon_\pm = \frac{\hbar^2 k^2}{2m} \mp \alpha_R k$, the magnetic case being described by eq. (8).

We can further proceed with a geometric analysis of our result, as illustrated in the Figure 3. We introduce the following contributions to the total (effective) magnetic field: (1) the Stoner field $\vec{B}_0 = \frac{2J_0}{g\mu_B}\vec{m}$ and (2) the Rashba field $\vec{B}_R \propto -\vec{k} \times \vec{E} = -\frac{2\alpha_R}{g\mu_B}\left(\vec{k} \times \vec{e}_z\right)$ that is perpendicular to the vectors ***k*** and ***E***; i.e. the Rashba field lies in (xoy) plane, and is perpendicular to the (**k**o**E**) plane.

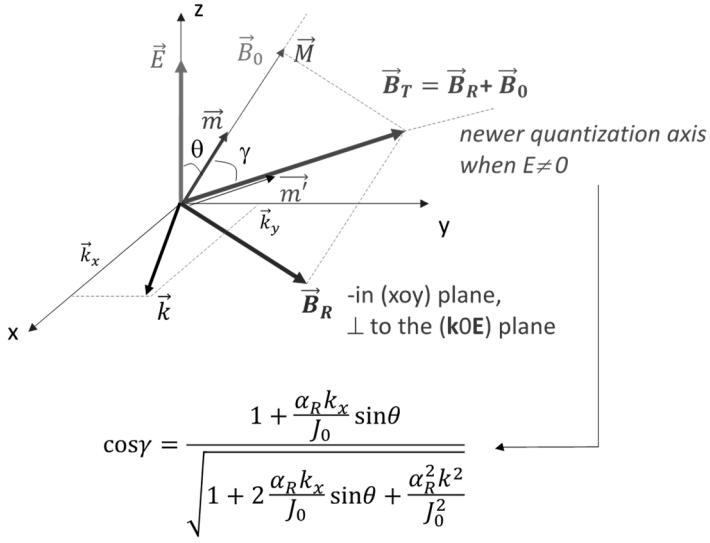

Figure 3. Geometric representation of the Stoner, Rashba and the effective field $\mathbf{B_T}$ whose new quantization direction is defined by the angle γ.

Then, the total (effective) magnetic field $\vec{B}_T = \vec{B}_R + \vec{B}_0$ will write:

$$\vec{B}_T = \vec{B}_0 \left[-\frac{\alpha_R k_y}{J_0} \vec{e}_x + \left(sin\theta + \frac{\alpha_R k_x}{J_0} \right) \vec{e}_y + \cos\theta \vec{e}_z \right] = \vec{B}_0 \overrightarrow{m'} \qquad (9)$$

In this equation, the $\overrightarrow{m'}$ will define the new direction of quantization direction corresponding to the case when an electric field is applied. It is issued from the competition between the Rashba field $\vec{B}_R$, perpendicular to ***E*** and **k,** and the exchange field $\vec{B}_0$. The magnetization dynamics related to the new direction of quantization direction generates the second order in ***E*** contribution to the anisotropy (last term in eq. 8) and is identified as a Dzyalozinskii-Moryia (DMI) interaction mechanism [11].

A partial conclusion can be driven in this point about the main result of the static eigenvalue analysis: the Rashba spin-orbit interaction is responsible on a uniaxial-anisotropy energy. That, within the Dzyaloshinskii-Moriya approach [11], includes a second order in electric field ***E*** in plane pseudo-dipolar interaction and another contribution proportional to $\boldsymbol{E^2/J_0 S}$, issued from the competition between the first order in ***E*** Rashba-Dzyaloshinskii-Moriya and the exchange fields. An effective $\boldsymbol{E^2}$ dependent perpendicular magnetic anisotropy may result in the situation when the Rashba-Dzyaloshinskii-Moriya term overcome the pseudo-dipolar ***E*** dependent one. Therefore, our simple Stoner-Rashba model, developed in the simplified case of quadratic free-electron dispersion framework, clearly indicates the interplay between the two terms in stabilizing the perpendicular magnetic anisotropy. We mention that the validity of results issued from this simplified free-electron approach has been further validated by band structure calculations [6] describing more accurately the localization of the wave-functions of 3d magnetic materials.

2. Rashba induced magnetization precession

From the static analysis, geometrically depicted in Figure 3, we saw that if initially (when ***E***=0) the magnetization quantization axis is $\overrightarrow{m}$, when the electric field ***E*** is switched on, due to the additional Rashba field $\mathbf{B_R}$, the newer quantization axis becomes $\overrightarrow{m'}$. Consequently, when the electric field is applied, the spin magnetization, initially aligned along the Stoner field $\mathbf{B_0}$ will not be any more in a stationary state, and a time evolution is expected. Using quantum mechanics time evolution analysis, we demonstrate and quantify that the magnetization will preces around the new quantization axis $\overrightarrow{m'}$.

We focus our analysis on a simplified situation, analytical easier to be calculated, when we fix the initial condition with the magnetization parallel to oz (plane of the 2DEG); m||oz (θ=0) that is the case of a sample with PMA.

Then, we calculate **the eigenvectors** corresponding to the $\varepsilon_{\pm}$ eigenvalues, the stationary solutions being (See Appendix 2):

$$|\Psi_{\varepsilon+}\rangle = e^{i\vec{k}\cdot\vec{r}}\left(\cos\frac{\gamma}{2}e^{\frac{i\varphi}{2}}|+\rangle - \sin\frac{\gamma}{2}e^{\frac{-i\varphi}{2}}|-\rangle\right)$$
$$|\Psi_{\varepsilon-}\rangle = e^{i\vec{k}\cdot\vec{r}}\left(\sin\frac{\gamma}{2}e^{\frac{i\varphi}{2}}|+\rangle + \cos\frac{\gamma}{2}e^{\frac{-i\varphi}{2}}|-\rangle\right) \quad (10)$$

The Hamiltonian being not explicitly dependent on time, the time dependence of the wave functions is simply introduced via some phase terms:

$$|\Psi(t)\rangle = C_+(0)e^{-\frac{i}{\hbar}\varepsilon_+ t}|\Psi_{\varepsilon+}\rangle + C_-(0)e^{-\frac{i}{\hbar}\varepsilon_- t}|\Psi_{\varepsilon-}\rangle \qquad \varepsilon_{\pm} = \frac{\hbar^2k^2}{2m} \mp \sqrt{J_0^2 + \alpha_R^2k^2}$$
$$C_+(t) = C_+(0)e^{-\frac{i}{\hbar}\varepsilon_+ t} \quad ; \quad (11)$$
$$C_-(t) = C_-(0)e^{-\frac{i}{\hbar}\varepsilon_- t}$$

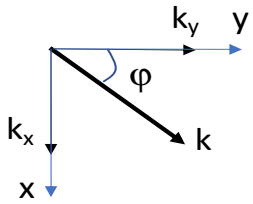

Figure 4

In-plane wave-vector of an electron in a 2DEG.

These time-dependent wave vectors are further used to calculate the average (expectation) value of the spin operators: $\langle\hat{S}_x\rangle, \langle\hat{S}_y\rangle, \langle\hat{S}_z\rangle$.

Within the Dirac formalism, the average (expectation) value of an operator is:

$$\langle A\rangle = \langle\Psi(t)|\boldsymbol{A}|\Psi(t)\rangle \quad (12)$$

With the *bra* and *ket* wave-vectors written as:

$$|\Psi(t)\rangle = \begin{pmatrix} C_+(t) \\ C_-(t) \end{pmatrix}; \quad \langle\Psi(t)| = (C_+^*(t) \quad C_-^*(t)) \quad (13)$$

Therefore, the average values will be:

$$\widehat{\langle S_x\rangle} = \hbar\Re e[C_+^*(t)C_-(t)]$$
$$\widehat{\langle S_y\rangle} = \hbar\Im m[C_+^*(t)C_-(t)] \quad (14)$$
$$\widehat{\langle S_z\rangle} = \frac{\hbar}{2}[C_+^*(t)C_+(t) - C_-^*(t)C_-(t)]$$

If initially, in a most general case the magnetization would make an angle δ with respect to ***m'*** (see Figure 5), we can write: $C_+(0) = \cos\frac{\delta}{2}; C_-(0) = \sin\frac{\delta}{2}$. When $\delta = -\gamma$ we find back the situation when, initially, **m**||oz.

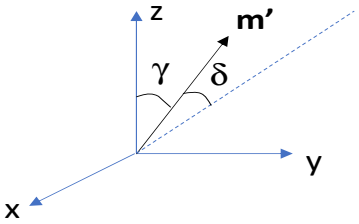

Figure 5

Initial geometry for the time-dependent analysis.

The calculations of the average values, after some simple math, leads to:

$$\begin{cases} \langle \hat{S}_x \rangle = \frac{\hbar}{2}\left[\cos^2\frac{\gamma}{2}\cos\left(\frac{2Jt}{\hbar}+\varphi\right) - \sin^2\frac{\gamma}{2}\cos\left(\frac{2Jt}{\hbar}-\varphi\right)\right] \\ \langle \hat{S}_y \rangle = -\frac{\hbar}{2}\left[cos^2\frac{\gamma}{2}sin\left(\frac{2Jt}{\hbar}+\varphi\right) + sin^2\frac{\gamma}{2}sin\left(\frac{2Jt}{\hbar}-\varphi\right)\right] \\ \langle \hat{S}_z \rangle = \frac{\hbar}{2}\left[\sin\gamma\cos\left(\frac{2Jt}{\hbar}\right)\right] \end{cases} \quad (15)$$

These set of three equations (15) describes the spin precession (and therefore the magnetization precession) around the ***m'*** direction, that is the quantization direction of the effective (total field, Rashba + Stoner): $\vec{\boldsymbol{B}}_{\boldsymbol{T}} = \vec{\boldsymbol{B}}_{\boldsymbol{R}} + \vec{\boldsymbol{B}}_{\boldsymbol{0}}$ described by a total **(**effective) molecular field:

$$J = J_{eff} = \sqrt{J_0^2 + \alpha^2 k^2} \quad (16)$$

The corresponding angular frequency (Larmor) for the precession will be:

$$\Omega = \frac{2J}{\hbar} = \frac{2\sqrt{J_0^2+\alpha^2k^2}}{\hbar} \quad (17)$$

Geometrically, this magnetization precession around the molecular total (effective) field is illustrated in Figure 6. One can see that the magnetization will preces with an angle equal to π (that would correspond to a toggle-like switch or reversal) if we apply a pulse of electric field with a time length equal to half of the Larmor period $t_{1/2} = \frac{T}{2} = \frac{\pi\hbar}{2\sqrt{J_0^2+\alpha^2k^2}}$. Therefore, under a pulse of perpendicular electric field applied to a magnetic 2D electron gas (that mimics an ultrathin magnetic film), we have a magnetization dynamic, similarly to a Nuclear Magnetic Resonance (NMR) experiment. Here, the ***E***-field, via the related Rashba magnetic field $\mathbf{B_R}$, plays the role of the radiofrequency (RF) in-plane magnetic field in NMR experiments.

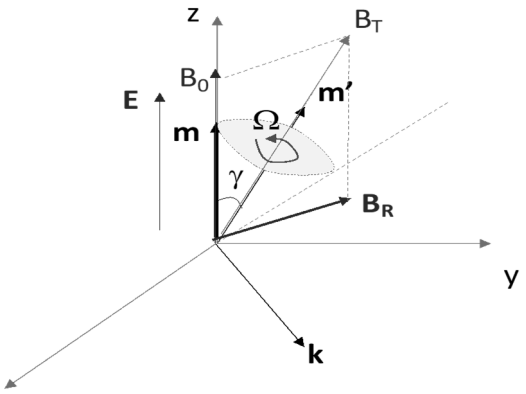

Figure 6

Magnetization precession around the molecular total field whose quantization direction is defined by ***m***'.

Our result indicates that NMR-like experiments can be successfully performed. Using pulses of laser, polarized with a component perpendicular to the film surface, the magnetization can be precesionally switched. However, more dedicated, and realistic experiments for the electric field toggling of the magnetization are commonly performed in lithographically patterned spintronic devices where a gating insulator is used for applying the field [12] or via the tunnel barrier in a magnetic tunnel junction) [13].

We can further add the following concluding remarks. The spin precession in external electric field is related to the spin-orbit interaction in the 2DEG (Rashba effect). The origin of this interaction is relativistic and has been addressed here using a "non-relativistic" Dirac Hamiltonian, deduced from the Dirac equation for a relativistic electron expanded to the lowest order in $(v/c)^2$. Note that even a classical relativistic *gedanken* analysis can phenomenologically explain the precession of a spin induced by an applied electric field. Therefore. an electron, moving with the velocity $\vec{v}$ in an external field $\vec{E}$, would "feel" in its own referential an effective magnetic field perpendicular on the direction of motion: $\vec{B} = -\frac{\vec{v}\times\vec{E}}{c^2}$. This magnetic field (i.e., Rashba field in our case) will lead to the spin Larmor precession.

Finally, we reiterate the important fact that the electric field used in our model can be either an external applied field, or, in realistic thin film heterostructures, an intrinsic electric field at the interface between a ferromagnetic ultrathin film and an insulator or a nonmagnetic metal with different workfunctions, or at the surface of the film due to the potential gradient related to the symmetry breaking. Independent of his origin, the existence of this electric field is responsible in ultrathin magnetic films on the perpendicular magnetic anisotropy [7]. We underline the fact that, in case of a surface or interface intrinsic electric field in multi-layered heterostructures, this field can be further modified by applying an external electric field. Moreover, as a function of the orientation of the external electric field, the intrinsic ***E***-field can be increased or decreased. Having in view the PMA dependence on the net electric

field felt by the 2DEG electrons, this would explain the possibility of controlling the anisotropy magnitude by the electric field (increase/decrease). In the literature, because the electric field is often generated by a biasing voltage, this phenomenon is called Voltage-Controlled-Magnetic-Anisotropy (VCMA) [14].

Beyond this simple quantum description, a more accurate study of the magnetization dynamics can be further performed within the Landau-Lifshitz-Gilbert (LLG) equation approach. That would consider the anisotropy energies, their dependence with respect to the electric field (that would affect the magnetic free-energy landscape), the phenomenological Gilbert damping contribution to the magnetization dynamics [8] and, beyond the macrospin approach, the micromagnetic features of ***E***-field toggling experiments in realistic patterned nanopillars based on ultrathin magnetic films.

CONCLUSIONS

Based on a Stoner-Rashba Hamiltonian approach, we underlined important static and dynamic issues related to the origin of the perpendicular magnetic anisotropy in ultrathin magnetic films, modelled as 2DEG magnetic systems. First, the static eigenvalue and eigenvector analysis show that the Rashba spin-orbit interaction leads to a uniaxial-anisotropy energy with a Stoner splitting, an in-plane pseudo-dipolar (proportional to the electric field **E**) and an out-of-plane ($\mathbf{E}^2$ dependent) competing contributions. Therefore, an effective perpendicular magnetic anisotropy may result when the Rashba-Dzyaloshinskii-Moriya term overcome the pseudo-dipolar one. Second, the time dependent analysis performed in case of the time-independent Stoner-Rashba Hamiltonian, illustrate that when an electric field is applied perpendicularly to the surface of the magnetic ultrathin film, the magnetization will preces around a new quantization axis corresponding to a net magnetic field resulting from vector sum of the initial Stoner field and the ***E***-field induced Rashba field. If the time length of a pulse of an applied electric field is equal to half of the Larmor precession period, magnetization toggling experiments NMR-like can be performed. Our results have been qualitatively confirmed and validated by more complex ab-initio and micromagnetic simulations that include more complex aspects.

ACKNOWLEDGEMENTS

C.T. acknowledges funding from the project «MODESKY» ID PN-III-P4-ID-PCE-2020-0230, No. UEFISCDI: PCE 245/02.11.2021. Moreover, the implementation of the current research further confirms and sustains the durability of previous funding projects: «SPINTRONIC» POS CCE Project: ID. 574, cod SMIS-CSNR 12467, «SPINTAIL» ID PN-II-PCE-2012-4-0315, No. UEFISCDI:23/29.08.2013 and «EMERSPIN» ID PN-III-P4-ID-PCE-2016-0143, No. UEFISCDI:22/12.07.2017.

APPENDIX 1:
THE SPIN-ORBIT HAMILTONIAN FOR A CENTRAL (SPHERICAL) POTENTIAL

The spin-orbit Dirac term that considers the spin-orbit interaction is obtained from the Dirac equation for a relativistic electron, expanded to the lowest order in $(v/c)^2$. Therefore, the non-relativistic Dirac Hamiltonian is:

$$H_{SO} = \frac{\hbar}{2m_0c^2}\vec{\nabla}V \cdot (\hat{\sigma} \times \hat{p})$$

Using some circular rules for the mixed vector product:

$$\vec{a} \cdot \left(\vec{b} \times \vec{c}\right) = \vec{b} \cdot (\vec{c} \times \vec{a}) = -\vec{b} \cdot (\vec{a} \times \vec{c})$$

we can rewrite:

$$H_{SO} = -\frac{\hbar}{2m_0c^2}\hat{\sigma} \cdot \left(\vec{\nabla}V \times \hat{p}\right) = -\frac{\hbar}{2m_0c^2}\left(\vec{\nabla}V \times \hat{p}\right) \cdot \hat{\sigma}$$

Moreover, for a spherical symmetry, the gradient *nabla* $\vec{\nabla}$ operator can be written in spherical coordinates as.

$$\vec{\nabla} = \frac{\partial}{\partial r}\hat{r} + \frac{1}{r}\frac{\partial}{\partial \theta}\hat{\theta} + \frac{1}{r\sin\theta}\frac{\partial}{\partial \varphi}\hat{\varphi}$$

In case of a central potential *V* having a spherical symmetry, *V* will only depend on *r* being independent on θ and φ. Thus, in this case:

$$\vec{\nabla}V = \frac{\partial V}{\partial r}\hat{r} = \frac{\partial V}{\partial r}\frac{\vec{r}}{r} = \frac{1}{r}\frac{\partial V}{\partial r}\vec{r}$$

This will lead to: $H_{SO} = -\frac{\hbar}{2m_0c^2}\frac{1}{r}\frac{\partial V}{\partial r}(\vec{r} \times \hat{p}) \cdot \hat{\sigma}$

In this equation, we recognize the orbital moment of the electron: $\vec{L} = \vec{r} \times \hat{p}$ whereas the Pauli spin operator $\hat{\sigma}$ is related to the spin momentum operator via $\hat{S} = \frac{\hbar}{2}\hat{\sigma}$. Within these circumstances:

$$H_{SO} = \lambda\vec{L} \cdot \vec{S}$$

with $\lambda = -\frac{1}{m_0c^2}\frac{1}{r}\frac{\partial V}{\partial r}$ the spin-orbit constant, proportional to the gradient of the potential (electric field). One can easily correlate the spin-orbit to λ coefficient and the Rashba constant $\alpha_R = \frac{\hbar^2}{2m_0c^2}\frac{\partial V}{\partial z}$, deduced in case of a non-spherical potential varying along the z direction perpendicular to the surface of a 2DEG. Beyond some constants, the most important common feature is their similar dependence on the potential gradient, so on the electric field.

APPENDIX 2:
THE STONER-RASHBA HAMILTONIAN MATRIX:
EIGENVALUES AND STATIONARY EIGENVECTORS

The Stoner-Rashba Hamiltonian is:

$$\hat{H} = \frac{\hat{p}^2}{2m} - J_0 \hat{m} \cdot \hat{\sigma} + \frac{\alpha_R}{\hbar}\left(\hat{\sigma}_x \hat{p}_y - \hat{\sigma}_y \hat{p}_x\right) = \frac{\hbar^2 \hat{k}^2}{2m} - J_0 \hat{m} \cdot \hat{\sigma} + \alpha_R\left(\hat{\sigma}_x \hat{k}_y - \hat{\sigma}_y \hat{k}_x\right)$$

and the Pauli matrices:

$$\hat{\sigma}_x = \begin{pmatrix} 0 & 1 \\ 1 & 0 \end{pmatrix}; \qquad \hat{\sigma}_y = \begin{pmatrix} 0 & -i \\ i & 0 \end{pmatrix}; \qquad \hat{\sigma}_z = \begin{pmatrix} 1 & 0 \\ 0 & -1 \end{pmatrix};$$

With $\{|i\rangle, |j\rangle\}$ belonging to the $\{|+\rangle, |-\rangle\}$ orthonormal basis $\langle i|j\rangle = \delta_{ij}$ (Kronecker *delta* symbol), one can calculate the matrix elements of the Hamiltonian $\hat{H}$:

$$\hat{H}_{ij} = \langle i|\hat{H}|j\rangle$$

For the free particle kinetic (first term) we get the diagonal Hamiltonian:

$$\hat{H}_{FP} = \begin{pmatrix} \dfrac{\hbar^2 \hat{k}^2}{2m} & 0 \\ 0 & \dfrac{\hbar^2 \hat{k}^2}{2m} \end{pmatrix}$$

For the Stoner term, we explicit the scalar product:

$$\vec{m} \cdot \hat{\sigma} = m_x \sigma_x + m_y \sigma_y + m_z \sigma_z = \sin\theta\, \sigma_y + \cos\theta\, \sigma_z,$$

in case when we consider a simplified configuration when $\varphi = \pi/2$ (Figure 1), so that $\hat{m}$ = (0, sinθ, cos θ)

Then, we get the explicit form for the Stoner term:

$$\hat{H}_S = -J_0\left(\sin\theta\, \sigma_y + \cos\theta\, \sigma_z\right)$$

Introducing the Pauli matrices, we get a Stoner Hamiltonian.

$$\hat{H}_S = -J_0 \begin{pmatrix} \cos\theta & -i\sin\theta \\ i\sin\theta & -\cos\theta \end{pmatrix}$$

Note that the Stoner Hamiltonian matrix is non-diagonal because the chosen magnetization direction θ does not correspond to the z quantization axis, initially considered for the definition of the Pauli matrices.

For the Rashba term $\hat{H}_R = \alpha_R\left(\hat{\sigma}_x \hat{k}_y - \hat{\sigma}_y \hat{k}_x\right)$ the matrix elements can be calculated by explicitly introducing the Pauli matrices definition:

$$\hat{H}_R = \alpha_R \begin{pmatrix} 0 & \hat{k}_y + i\hat{k}_x \\ \hat{k}_y - i\hat{k}_x & 0 \end{pmatrix}$$

Adding all the contributions, one finds that the matrix of the total Hamiltonian is:

$$\hat{H}_T = \begin{pmatrix} \frac{\hbar^2\hat{k}^2}{2m} - J_0\cos\theta & iJ_0\sin\theta + \alpha_R(\hat{k}_y + i\hat{k}_x) \\ -iJ_0\sin\theta + \alpha_R(\hat{k}_y - i\hat{k}_x) & \frac{\hbar^2\hat{k}^2}{2m} + J_0\cos\theta \end{pmatrix}$$

One can observe that the Hamiltonian matrix is non-diagonal, therefore the $|+\rangle$ and $|-\rangle$ states are not eigenstates of the Hamiltonian (system).

The eigenvalues can be calculated by solving the linear algebra eigenvalues equation:

$$\det(\hat{H}_T - \lambda\hat{I}) = 0$$

where $\hat{I} = \begin{pmatrix} 1 & 0 \\ 0 & 1 \end{pmatrix}$ is the unit 2×2 matrix.

Some elementary algebra leads to:

$$\lambda_{1,2} = \varepsilon_{\pm} = \frac{\hbar^2k^2}{2m} \mp \sqrt{J_0^2 + 2J_0\alpha_R k_x \sin\theta + \alpha_R^2 k^2}\,;$$

with $\sigma = \pm 1$ (up, dn) and $k = (k_x, k_y, 0)$.

The eigenvectors corresponding to these eigenvalues are calculated from the linear algebra equation:

$$(\hat{H}_T - \lambda\hat{I})\begin{pmatrix} u \\ v \end{pmatrix} = 0$$

with $\lambda_{1,2} = \varepsilon_{\pm}$.

Some elementary algebra leads to the stationary eigenvectors:

$$|\Psi_{\varepsilon+}\rangle = e^{i\vec{k}\cdot\vec{r}}\left(\cos\frac{\gamma}{2}e^{\frac{i\varphi}{2}}|+\rangle - \sin\frac{\gamma}{2}e^{\frac{-i\varphi}{2}}|-\rangle\right)$$

$$|\Psi_{\varepsilon-}\rangle = e^{i\vec{k}\cdot\vec{r}}\left(\sin\frac{\gamma}{2}e^{\frac{i\varphi}{2}}|+\rangle + \cos\frac{\gamma}{2}e^{\frac{-i\varphi}{2}}|-\rangle\right)$$

The phase factor φ is related to the in-plane orientation of the wave vector k.

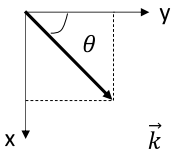

$$k_y = k\cos\varphi \qquad k_x + ik_y = e^{i\varphi}k$$
$$k_y = k\sin\varphi \qquad k_x - ik_y = e^{i\varphi}k$$

Figure A2.1 Geometrical interpretation of the phase factor φ

REFERENCES

1. B. Dieny, M. Chshiev, *Rev. of Mod. Phys.,* vol. 89, (2017).
2. D. C. M. Yamanouchi, F. Matsukura, H. Ohno, *Science*, 301, 943-945 (2003).
3. S. Kanai, F. Matsukura, H. Ohno, *Appl. Phys. Lett.*, 108, 192406 (2016).
4. C. Grezes, F. Ebrahimi , J. G. Alzate, X. Cai, J. A. Katine , J. Langer, B. Ocker , P. Khalili Amiri, K. L. Wang, *Appl. Phys. Lett.,* 108, 012403 (2016).
5. E. G. V. Krizakova, G. Sala, F. Yasin , S. Couet, G. S. Kar, K. Garello, P. Gambardella, *Nature Nanotechnology*, 15, 111 (2020).
6. R-A. One, S. Mican, C. Tiusan, *Stud. Univ. Babeș- Bolyai Phys*. 66, 91–110 (2021).
7. F. Ibrahim, H. Yang, A. Halla, M. Chshiev, *Phys. Rev. B*, 93, 014429 (2016).
8. R-A. One, H. Béa, S. Mican, M. Joldos, P. Brandão Veiga, B. Dieny, L. D. Buda-Prejbeanu & C. Tiusan, *Sci Rep* 11, 8801 (2021).
9. A. Manchon, S. Zhang, *Phys. Rev. B* 79, 094422 (2009).
10. S. E. Barnes, J. Ieda, S. Maekawa, *Sci. Rep.*, 4, 4105 (2015).
11. I. E. A. Dzyaloshinskii, *J. Chem. Solids* 4, 241–255 (1958); T. Moriya, *Phys. Rev.* 120, 91–98 (1960); T. Moriya, *Phys. Rev. Lett.* 4, 228–230 (1960).
12. R-A One, S Mican, A Mesaros, M Gabor, T Petrisor, M Joldos, LD Buda-Prejbeanu, C Tiusan, *IEEE Trans. on Magn.* 57(6), (2021).
13. S. Kanai, F. Matsukura, & H. Ohno, , *Appl. Phys. Lett.* 108, 192406 (2016).
14. J. Zhang, P. V. Lukasev, S. S. Jaswal, & E. Y. Tsymbal, *Phys. Rev. B* 96, 014435 (2017).